Bioorganic & Medicinal Chemistry 18 (2010) 5316–5322

Contents lists available at ScienceDirect

Bioorganic & Medicinal Chemistry

journal homepage: www.elsevier.com/locate/bmc

Novel anti-viability ceramide analogs: Design, synthesis, and structure–activity relationship studies of substituted (*S*)-2-(benzylideneamino)-3-hydroxy-*N*-tetradecylpropanamides

Jiawang Liu [†], James W. Antoon [‡], Adharsh Ponnapakkam [‡], Barbara S. Beckman [‡], Maryam Foroozesh [*,†]

Department of Chemistry, Xavier University of Louisiana, 1 Drexel Drive, New Orleans, LA 70125, USA
Department of Pharmacology, Tulane University School of Medicine, 1430 Tulane Avenue, New Orleans, LA 70112, USA

ARTICLE INFO

Article history:
Received 15 December 2009
Revised 14 May 2010
Accepted 16 May 2010
Available online 8 June 2010

Keywords:
Ceramide
Sphingosine-1-phosphate
MTT viability assay
Partial atomic charge
Resonance
Inductive effects
Structure–activity relationship

ABSTRACT

A group of novel L-serinamides, substituted (*S*)-2-(benzylideneamino)-3-hydroxy-*N*-tetradecylpropanamides (**3a–o**) and substituted (*S*)-2-(benzylamino)-3-hydroxy-*N*-tetradecyl propanamides (**4c**, **4i**, **4l**, and **4o**), were synthesized as potential anti-tumor lead compounds. In vitro cell viability assay results indicate treatment with **3a–o** compounds resulted in significant inhibition of cell viability in the chemo-resistant breast cancer cell line, MCF-7TN-R. Compounds **3i** and **3l**, both *ortho*-substituted analogs, show the greatest efficacy with IC_{50} values of 10.3 μM and 12.5 μM, respectively. The SAR analysis indicate that the imine functional group of **3a–o** is critical for the cellular anti-viability effect, and the partial atomic charge (PAC) value of imine C atom is a valuable structural parameter for predicting the activity of these ceramide analogs.

1. Introduction

Recent research suggests that bioactive sphingolipids play an important role in the regulation of cancer pathogenesis and provide novel clues towards the discovery of new chemotherapeutic agents.[1–3] The central molecule in the sphingolipid metabolism, ceramide, is known to induce apoptosis,[4] senescence[5,6] and growth arrest[7] in many human cancers. Ceramide could be metabolized into sphingosine-1-phosphate (S-1-P) by the successive actions of the enzymes ceramidase (CDase) and sphingosine kinase (SK). This metabolite, however, causes cellular transformation, decreased apoptosis, and induction of angiogenesis.[1,2] Therefore, many researchers have focused on designing ceramide analogs with the same apoptotic activity as ceramide but with greater inhibitory effect on the enzymes involved in ceramide metabolism, leading to the synthesis of dozens of active molecules recently reported.[8–13] In fact, decreased synthesis and increased metabolism of ceramide has already become an important target of anti-cancer agents. Figure 1 illustrates the probable mechanism of action of ceramide analogs.

L-Serinamides,[14,15] serinol,[16] and aminoethanol amide[17,18] have been previously investigated as anti-cancer ceramide analogs. We have recently reported that a series of ceramide analogs based on the structure of L-serine amide, particularly (*S*)-2-(benzylideneamino)-3-hydroxy-*N*-tetradecylpropanamide (analog **3**, IC_{50}, 7.67 μM), exhibit increased efficacy as anti-proliferative agents in both chemosensitive and chemoresistant breast cancer cell lines compared to the parent compound (C8-ceramide, IC_{50}, 8.59 μM).[9] This compound is able to alter the sphingolipid metabolism profile of both chemosensitive and chemoresistant breast cancer cells causing a significant increase in sphinganine levels while diminishing intracellular S1P protein concentrations.

Using (*S*)-2-(benzylideneamino)-3-hydroxy-*N*-tetradecylpropanamide (Analog 3) as the lead, we incorporated five functional groups (–NO_2, –CH_3, –Cl, –OCH_3, and –OH) into each position (*ortho*-, *meta*-, and *para*-) of the benzyl group in order to alter electronic properties of the imine group, the metabolism-relevant functional group. The position of the substituent (*o*-, *m*-, *p*-), Log *K* (representing lipid–water partition coefficient), electron-withdrawing or electron-releasing ability, and molecular weight (molecular size) were taken in consideration as parameters for the investigation of the structure–activity relationships. Nineteen analogs were synthesized and assayed for their effects on cell viability in chemo-resistant (MCF-7TN-R) breast cancer cell line. The MCF-7TN-R cell line was derived from MCF-7 cells grown in

* Corresponding author. Tel.: +1 504 520 5078.
E-mail address: mforooze@xula.edu (M. Foroozesh).
† Xavier University of Louisiana, Department of Chemistry, USA.
‡ Tulane University, School of Medicine, USA.

0968-0896/$ - see front matter © 2010 Elsevier Ltd. All rights reserved.
doi:10.1016/j.bmc.2010.05.044

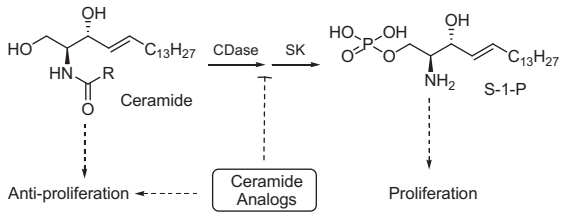

Figure 1. The expected mechanism of action of ceramide analogs. Ceramidase (CDase), sphingosine kinase (SK), sphingosine-1-phosphate (S-1-P).

increasing concentrations of tumor necrosis factor α (TNF-α) until resistance was established.[19] Using in vitro assays, **3i** and **3l**, both *o*-substituted analogs, showed the greatest efficacy with IC_{50} values of 10.3 and 12.5 μM, respectively. The partial atomic charges (PAC)[20] of metabolism-relevant N and C atoms of the imine group were calculated in CERIUS^2, and the results indicate that the PAC of the C atom of the imine functional group is relevant to the viability inhibition of MCF-7TN-R cell line (Table 1). Given the need for experimental therapeutics to exhibit at least a modest selectivity for cancer rather than normal cells, we analyzed the effect of these ceramide analogs on the non-tumorigenic HEK294 kidney cell line (Table 2). Most analogs showed higher potency in the cancer cell line, with the exceptions of analog **3a**, **3b**, **3d**, **3e**, and **3f**. Interestingly, the analogs **3i** and **3l** which have shown the highest potency against breast cancer cells also show the highest degree of selectivity.

2. Results and discussion

2.1. Synthesis

The synthetic route of ceramide analogs is depicted in Scheme 1. Boc-L-serine was coupled with tetradecylamine giving Boc-L-serinamide in 92% yield. After removing the Boc protecting group with trifluoroacetic acid in dichloromethane, L-serinamide was formed in 66% yield. In the presence of sodium hydroxide, **3a–o** were formed in methanol, and crystals were obtained by recrystallization from petroleum ether/ethyl acetate (**3a–l**) and petroleum ether/methanol (**3m–o**) solvent systems. Reduction of **3c**, **3i**, **3l** and **3o** by $NaBH_4$ provided (*S*)-2-(benzylamino)-3-hydroxy-*N*-tetradecyl propanamides **4c**, **4i**, **4l**, and **4o** in 73–78% yields. All of these reactions occurred in mild conditions, and ceramide analogs were produced in acceptable yields.

Table 2
IC_{50} values of **3a–o** in a non-tumorigenic human kidney cell line (HEK294)

Compd	IC_{50} (μM)
3a	49.51
3b	82.66
3c	82.61
3d	47.32
3e	51.11
3f	81.06
3g	77.69
3h	76.96
3i	94.88
3j	81.65
3k	77.26
3l	79.15
3m	71.68
3n	77.52
3o	80.78

2.2. Anti-viability effects of compounds 3a–o in MCF-7TN-R chemoresistant breast cancer cells and HEK294 non-tumorigenic kidney cells

The effects of compounds **3a–o** on the viability of MCF-7TN-R cells were assessed by means of MTT assays according to previously published methods.[9] Among the fifteen imine analogs, **3i** and **3l**, with *o*-chloro- and *o*-methoxy-substituents, showed the greatest anti-viability effect with IC_{50} values of 10.3 and 12.5 μM, respectively. (Table 1, Fig. 2). Most analogs showed higher potency in the cancer cell line, with the exceptions of analogs **3a**, **3b**, **3d**, **3e**, and **3f**. IC_{50}s ranged from 47.32 to 94.88 μM (Table 2).

2.3. Structure–activity relationship studies of compounds 3a–o

The structural parameters of **3a–o** are listed in Table 1. Due to the structural similarity of these compounds, molecular weight could be treated as a parameter of molecular size. Partial atomic

Table 1
Structural parameters and IC_{50} values of **3a-o** and **4c**,**4i**,**4l**,**4o**

Compd	Group	Position	MW	Log *K*	Log *P* (predicted)	PAC (N)	PAC (C)	IC_{50} (μM)
C8-Cer[a]								8.59[c]
3[b]								7.67[c]
3a	$-NO_2$	*para*-	433.5	0.86	5.59	−0.2768	0.0295	216.5
3b	$-NO_2$	*meta*-	433.5	0.86	5.59	−0.2768	0.0297	103.9
3c	$-NO_2$	*ortho*-	433.5	0.88	5.56	−0.2767	0.0337	21.71
3d	$-CH_3$	*para*-	402.6	1.09	6.37	−0.2768	0.0295	101.5
3e	$-CH_3$	*meta*-	402.6	1.09	6.37	−0.2768	0.0295	82.94
3f	$-CH_3$	*ortho*-	402.6	1.09	6.20	−0.2768	0.0298	87.71
3g	−Cl	*para*-	423.0	1.09	6.59	−0.2768	0.0295	27.48
3h	−Cl	*meta*-	423.0	1.08	6.59	−0.2768	0.0296	24.10
3i	−Cl	*ortho*-	423.0	1.12	6.43	−0.2768	0.0310	10.26
3j	$-OCH_3$	*para*-	418.6	0.91	5.94	−0.2768	0.0295	28.13
3k	$-OCH_3$	*meta*-	418.6	0.92	5.94	−0.2768	0.0296	31.25
3l	$-OCH_3$	*ortho*-	418.6	0.89	5.96	−0.2767	0.0322	12.50
3m	−OH	*para*-	404.5	0.73	5.67	−0.2768	0.0295	19.33
3n	−OH	*meta*-	404.5	0.76	5.67	−0.2768	0.0296	32.63
3o	−OH	*ortho*-	404.5	0.89	5.70	−0.2767	0.0322	18.97
4c	$-NO_2$	*ortho*-	435.5	0.28	4.92	−0.2997	0.0255	29.35
4i	−Cl	*ortho*-	425.0	0.27	5.79	−0.2998	0.0288	43.69
4l	$-OCH_3$	*ortho*-	420.6	0.27	5.32	−0.2997	0.0239	100.4
4o	−OH	*ortho*-	406.8	0.22	5.06	−0.2997	0.0239	75.29

[a] C8-ceramide.
[b] Analog **3**.
[c] Data of clonogenic survival assay previously, Ref. 9.

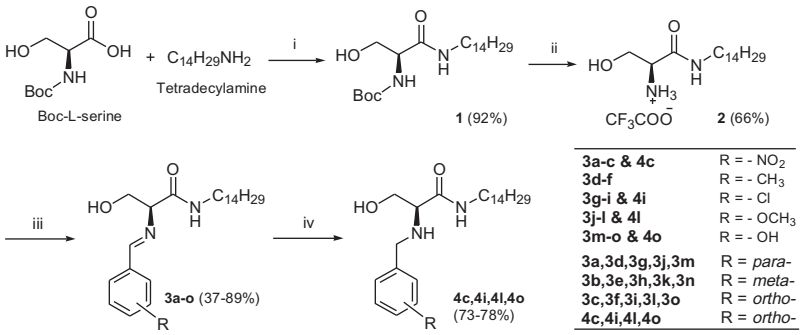

Scheme 1. Synthesis of **3a**–**o** and **4c**, **4i**, **4l**, **4o**. Reagents and conditions: (i) DCC/HOBT in THF 0 °C; (ii) TFA/CH_2Cl_2 (0 °C); (iii) NaOH in methanol, and various substituted benzaldehydes; (iv) $NaBH_4$/methanol.

charge (PAC) as an electronic descriptor, quantifies the charges in a local electric field surrounding the nucleus of an atom. The PAC values of atoms N and C of the imine functional group were calculated in Cerius[2] (Accelrys Software Inc., San Diego, California), since the imine group is the key site of hydrolysis in ceramide metabolism. The 3D structures of **3a–o** were sketched in ISIS Draw (Symyx Technologies, Inc.), and energetically minimized in Cerius[2] 4.11. The partial atomic charges were assigned using the Gasteiger method.[21–23] The data show that almost no difference exists in PAC (N) values among **3a–o**, however, a significant rise in electropositivity of the carbon atom occurs in the *o*-substituted analogs except the compound possessing an *o*-methyl group **3f**.

It is well known that Log *K* value of a compound is highly correlated with the corresponding Log *P* value, and it is treated as a parameter that represents the lipid/water partition coefficient. Log *K* values of **3a**–**o** were calculated using retention times obtained from RP-HPLC analysis. Predicted Log *P* values are also displayed in Table 1, which were calculated in the QSAR (quantitative structure–activity relationship) module of Cerius[2], after regular energy minimization, and charge distribution employing Merck Molecular Force Field. As is shown in Table 1, the analogs with the same substituent possess the similar Log *K* values except hydroxy-substituted compounds. The Log *K* value of *o*-hydroxy-substituted analog **3o** is significantly higher than the values of its *p*- and *m*-substituted counterparts **3m** and **3n**, which may be attributed to the formation of intramolecular hydrogen bond in **3o**. However, no correlation was observed between Log *K* and anti-viability effect in this study.

2.4. Activity of the analogs with same substituted position

Among the *p*-substituted analogs, **3g** (27.48 μM), **3j** (28.13 μM), and **3m** (19.33 μM) were more effective than **3a** (216.5 μM) and **3d** (101.5 μM) in IC_{50} values. Analogs **3g**, **3j**, **3m**, respectively, contain chloro, methoxy, and hydroxy groups which donate electrons by resonance but withdraw electrons by inductive effect. However, the substituent of analog **3a** (nitro), is an electron-withdrawing group (EWG) both by inductive effect and resonance, and substituent of analog **3d** (methyl), is an electron-donating group (EDG) only by inductive effect. This observation indicates that the electron-donating effect by resonance accounts for the relatively high activity of these compounds. A similar trend was observed among the m-substituted analogs **3b**, **3e**, **3h**, **3k**, and **3n**. However, in the *o*-substituted analogs, **3f (*o*-methyl)** containing EDG only by inductive effect, showed less efficacy than the other compounds, **3c (*o*-nitro), 3i (*o*-chloro), 3l (*o*-methoxy),** and **3o (*o*-hydroxy).** This suggests that electron-withdrawing by inductive effect, rather than by resonance, will enhance the anti-viability activity of o-substituted analogs.

2.5. *o*-Substitution versus partial atomic charge of the imine carbon

We further compared the analogs containing the same type of substituents and found a notable increase of anti-viability activity in *o*-substituted compounds, except for the analog with methyl group **3f**. At the same time, a similar increase in electro positivity of the carbon atom was observed in these analogs. As described above, anti-viability effect correlates with electron-withdrawing effect by induction at *o*-position. Analogs, **3c** (*o*-nitro), **3i** (*o*-chloro), **3l** (*o*-methoxy), and **3o** (*o*-hydroxy) with EWGs by inductive effect, withdraw electrons from the carbon atom of the imine group and subsequently increase the PAC (C) value as well as the anti-viability activity, while analog **3f** (*o*-methyl) with EDG by inductive effect works in an opposite manner. This finding suggests that the electronic charge distribution of the imine functional group is critical for increased activity and PAC (C) value could be used as a useful indicator of activity in future studies.

2.6. The effect of 4c, 4i, 4l, and 4o on the cell viability in MCF-7TN-R cells

In order to investigate the importance of carbon–nitrogen double bond on anti-viability activity, the four most effective *o*-substituted analogs **3c**, **3i**, **3l**, and **3o** were reduced to form compounds **4c**, **4i**, **4l**, and **4o**. The effects of compounds **4c**, **4i**, **4l**, and **4o** on the viability of MCF-7TN-R cells were also determined by MTT assays. A series of relatively high IC_{50} values were obtained with 29.35 μM, 43.69 μM, 100.4 μM, 75.29 μM for **4c**, **4i**, **4l**, and **4o**, respectively (Table 1). The decline of activity brought by introducing carbon–nitrogen single bond indicates that the conjugated system composed by the imine functional group (C=N) and phenyl ring is critical for the observed anti-viability effect. In addition, the relatively low PAC (C) values of **4c**, **4i**, **4l**, and **4o** may also account for the decrease in activity compared to their imine counterparts.

3. Conclusions

Nineteen ceramide analogs were designed and synthesized using fifteen benzaldehydes as starting material in acceptable yields. Five different substituents were incorporated into each position of the phenyl ring (*o*, *m*, *p*) in order to determine the most effective combination of substituent and position. These analogs were tested as potential anti-viability agents in MCF-7TN-R cells, and the structure–activity relationships were studied using several parameters. The results indicate that all analogs containing chloro-, methoxy-, and hydroxyl- substituents show great efficacy. In analogs containing a methyl group, a significant increase of the PAC (C) in the *o*-substituted compound was detected, which may

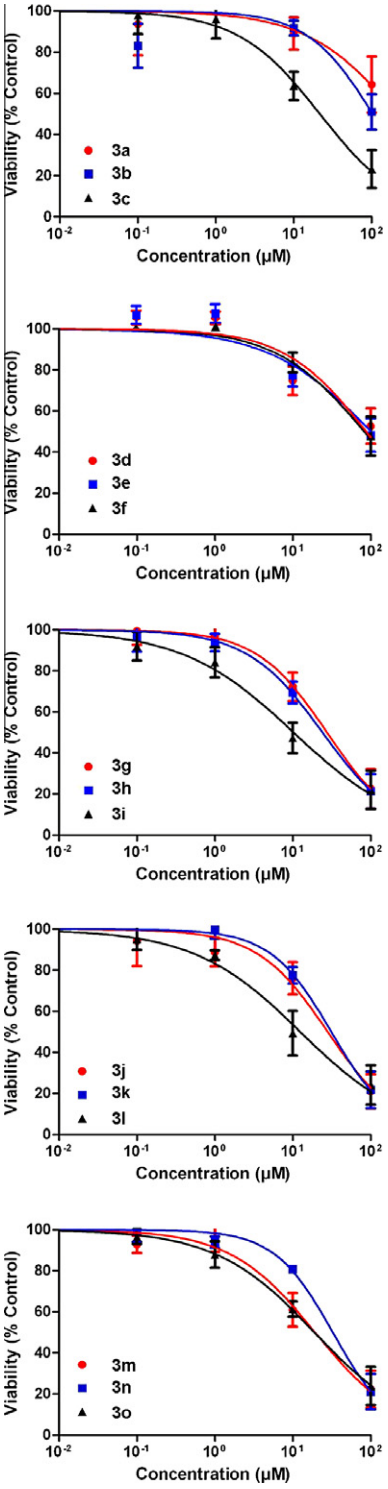

Figure 2. Effect of compounds **3a**–**n** on breast cancer viability in MCF-7TN-R cells. MCF-7TN-R cells were plated at 7.5×10^5 cells per 96 well plate. The following day cells were treated with indicated concentrations of compound for 24 h. Data are presented as percent of vehicle treated samples. Mean values of ±S.E.M. of four different experiments in quadruplicate are reported.

account for the increased anti-viability activity. Therefore, *ortho*-substituted analogs with electron withdrawing groups by induction seem to be the best choice for further research, and PAC (C) seems to be a valuable predictor of the structural property of the molecule to be used in our future QSAR analysis of ceramide analogs. While comparing imine and amine functional groups, we found that the relatively high activity of the imine functional group is most likely due to the stability of the π–Π conjugation at the hydrolytic site of the enzymes involved. These analogs were also tested as potential anti-viability agents in non-tumorigenic human kidney cell line HEK294, and the results showed that the most potent analogs in breast cancer cells are also the most selective. In conclusion, our study illustrates that targeting ceramide analogs for chemotherapeutic drug design has potential in treating drug resistant breast cancer.

4. Experimental section

4.1. Chemistry

All the chemicals were purchased from Sigma–Aldrich Chemical Co. (St. Louis, MO). Chromatography was performed on HPTLC Silica Gel 60 F_{254}, and RP-HPLC was performed on *hp* Hewlett Packard Series 1050 (Column: phenomenex Gemini-NX 5u C18 110A). The amino acid analysis was determined with a Hitachi 835-50 instrument. Mass spectral data was determined by Micromass Quattro *micro*™ API and Agilent 6890 GC with 5973 MS. ^{1}H NMR and ^{13}C NMR spectra were recorded on Varian 300 MHz NMR spectrometer.

4.1.1. (*S*)-*tert*-Butyl 3-hydroxy-1-oxo-1-(tetradecylamino) propan-2-ylcarbamate (1)

Compound **1** was prepared according to the literature.[9]

4.1.2. (*S*)-2-Amino-3-hydroxy-*N*-tetradecylpropanamide (2)

Compound **2** was prepared according to the literature.[9]

4.1.3. General procedure for synthesis of nitro-, methyl-, chloro- and methoxy-substituted (*S*)-2-(benzylideneamino)-3-hydroxy-*N*-tetradecylpropanamide (3a–l)

A mixture of 0.40 g (1.00 mmol) of (*S*)-2-amino-3-hydroxy-*N*-tetradecylpropanamide hydrochloride, 0.04 g (1.00 mmol) of NaOH, 1.00 mmol of substituted benzaldehyde, and 40 mL of methanol was stirred at room temperature for eight hours. The solvent was then evaporated under reduced pressure, and the residue was dissolved in 60 mL of ethyl acetate. After filtration and evaporation, the residue was washed four times with 10 mL of petroleum ether and 20 mL of cold methanol (4 °C) to get the crude products. The substituted (*S*)-2-(benzylideneamino)-3-hydroxy-*N*-tetradecylpropanamides (**3a–l**) were obtained by recrystallization from petroleum ether/ethyl acetate.

4.1.3.1. (*S*)-2-(4-Nitrobenzylideneamino)-3-hydroxy-*N*-tetradecylpropanamide (3a). Yield: 0.18 g (42%) as colorless powder. GC/MS (*m*/*e*): 434 $[M+1]^+$, 317 $[M+1-OH]^+$, ^{1}H NMR (DMSO-d_6, 300 MHz) δ/ppm = 8.416 (s, 1H), 8.297 (d, J = 8.7 Hz, 2H), 8.125 (d, J = 8.7 Hz, 2H), 7.800 (t, J = 5.7 Hz, 1H), 4.913 (t, J = 6 Hz, 1H), 3.866 (m, 2H), 3.504 (m, 1H), 3.084 (m, 2H), 1.391 (m, 2H), 1.176 (m, 22H), 0.826 (t, J = 6 Hz, 3H). ^{13}C NMR (DMSO-d_6, 75 MHz) δ/ppm = 169.996, 161.706, 149.362, 142.104, 131.339, 124.415, 76.466, 63.621, 39.115, 31.964, 29.808, 29.632, 29.686, 29.398, 26.999, 22.763, 14.609. Anal. Calcd for $C_{24}H_{39}N_3O_4$: C, 66.48; H, 9.07; N, 9.69; O, 14.76. Found: C 66.44; H, 9.65; N, 9.52; O, 14.34.

4.1.3.2. (*S*)-2-(3-Nitrobenzylideneamino)-3-hydroxy-*N*-tetradecylpropanamide (3b). Yield: 0.22 g (51%) as colorless powder. GC/MS (*m*/*e*): 433 M^+, ^{1}H NMR (DMSO-d_6, 300 MHz) δ/ppm = 8.671 (s, 1H), 8.421 (s, 1H), 8.291 (m, 2H), 7.784 (m, 2H), 4.907 (t, J = 6 Hz, 1H), 3.869 (m, 2H), 3.520 (m, 1H), 3.081 (m, 2H), 1.389 (m, 2H), 1.176 (m, 22H), 0.825 (t, J = 6 Hz, 3H). ^{13}C NMR (DMSO-d_6, 75 MHz) δ/ppm = 170.087, 161.539, 148.830, 138.126, 135.545, 130.929, 125.918, 123.003, 76.405, 63.636, 39.100, 31.964, 29.808, 29.671, 29.701, 29.382, 26.999, 22.778,

14.609. Anal. Calcd for $C_{24}H_{39}N_3O_4$: C, 66.48; H, 9.07; N, 9.69; O, 14.76. Found: C 66.23; H, 8.93; N, 9.62; O, 14.45.

4.1.3.3. (*S*)-2-(2-Nitrobenzylideneamino)-3-hydroxy-*N*-tetradecylpropanamide (3c). Yield: 0.38 g (89%) as yellow powder. GC/MS (*m*/*e*): 434 $[M+1]^+$, ^{1}H NMR (DMSO-d_6, 300 MHz) δ/ppm = 8.543 (s, 1H), 8.187 (d, J = 7.5 Hz, 1H), 8.028 (d, J = 7.5 Hz, 1H), 7.805 (t, J = 7.5 Hz, 1H), 7.720 (t, J = 7.5 Hz, 1H), 7.611 (t, J = 5.7 Hz, 1H), 4.855 (t, J = 6 Hz, 1H), 3.903 (dd, J = 3.9 Hz, J = 8.1 Hz, 1H), 3.793 (m, 1H), 3.506 (m, 1H), 3.084 (m, 2H), 1.397 (m, 2H), 1.198 (m, 22H), 0.832 (t, J = 6 Hz, 3H). ^{13}C NMR (DMSO-d_6, 75 MHz) δ/ppm = 169.905, 159.018, 149.665, 142.104, 133.981, 132.295, 130.656, 124.764, 76.329, 63.636, 39.100, 31.979, 29.808, 29.701, 29.641, 29.382, 26.968, 22.778, 14.624. Anal. Calcd for $C_{24}H_{39}N_3O_4$: C, 66.48; H, 9.07; N, 9.69; O, 14.76. Found: C 66.59; H, 9.08; N, 9.28; O, 14.69.

4.1.3.4. (*S*)-2-(4-Methylbenzylideneamino)-3-hydroxy-*N*-tetradecylpropanamide (3d). Yield: 0.24 g (60%) as colorless powder. GC/MS (*m*/*e*): 402 M^+, 385 $[M-\cdot OH]^+$, ^{1}H NMR (DMSO-d_6, 300 MHz) δ/ppm = 8.215 (s, 1H), 7.705 (m, 3H), 7.253 (d, J = 8.1 Hz, 2H), 4.808 (t, J = 6 Hz, 1H), 3.769 (m, 2H), 3.466 (m, 1H), 3.067 (m, 2H), 2.336 (s, 3H), 1.385 (m, 2H), 1.194 (m, 22H), 0.833 (t, J = 6 Hz, 3H). ^{13}C NMR (DMSO-d_6, 75 MHz) δ/ppm = 170.588, 163.011, 141.405, 134.011, 129.775, 129.061, 76.254, 63.834, 39.024, 31.994, 29.823, 29.732, 29.413, 26.999, 22.778, 21.760, 14.609. Anal. Calcd for $C_{25}H_{42}N_2O_2$: C, 74.58; H, 10.51; N, 6.96; O, 7.95. Found: C 72.67; H, 10.41; N, 7.29; O, 8.78.

4.1.3.5. (*S*)-2-(3-Methylbenzylideneamino)-3-hydroxy-*N*-tetradecylpropanamide (3e). Yield: 0.31 g (77%) as colorless powder. GC/MS (*m*/*e*): 402 M^+, 385 $[M-OH]^+$, ^{1}H NMR (DMSO-d_6, 300 MHz) δ/ppm = 8.223 (s, 1H), 7.686 (m, 2H), 7.595 (d, J = 7.2 Hz, 1H), 7.306 (m, 2H), 4.823 (t, J = 6 Hz, 1H), 3.790 (m, 2H), 3.479 (m, 1H), 3.080 (m, 2H), 2.342 (s, 3H), 1.387 (m, 2H), 1.203 (m, 22H), 0.833 (t, J = 6 Hz, 3H). ^{13}C NMR (DMSO-d_6, 75 MHz) δ/ppm = 170.542, 163.330, 138.445, 136.501, 132.250, 129.228, 129.107, 126.586, 76.345, 63.788, 39.024, 31.979, 29.808, 29.701, 29.398, 26.999, 22.778, 21.533, 14.624. Anal. Calcd for $C_{25}H_{42}N_2O_2$: C, 74.58; H, 10.51; N, 6.96; O, 7.95. Found: C 73.37; H, 10.40; N, 7.05; O, 8.21.

4.1.3.6. (*S*)-2-(2-Methylbenzylideneamino)-3-hydroxy-*N*-tetradecylpropanamide (3f). Yield: 0.30 g (74%) as colorless powder. GC/MS (*m*/*e*): 402 M^+, 385 $[M-OH]^+$, ^{1}H NMR (DMSO-d_6, 300 MHz) δ/ppm = 8.527 (s, 1H), 7.949 (d, J = 7.5 Hz, 1H), 7.642 (d, J = 5.7 Hz, 1H), 7.261 (m, 3H), 4.814 (t, J = 6 Hz, 1H), 3.825 (m, 2H), 3.475 (m, 1H), 3.092 (m, 2H), 2.466 (s, 3H), 1.391 (m, 2H), 1.196 (m, 22H), 0.831 (t, J = 6 Hz, 3H). ^{13}C NMR (DMSO-d_6, 75 MHz) δ/ppm = 170.573, 161.918, 138.399, 134.436, 131.384, 131.096, 128.272, 126.526, 76.694, 63.803, 39.024, 31.994, 29.838, 29.747, 29.428, 27.014, 22.793, 19.604, 14.594. Anal. Calcd for $C_{25}H_{42}N_2O_2$: C, 74.58; H, 10.51; N, 6.96; O, 7.95. Found: C 73.10; H, 10.46; N, 6.89; O, 9.11.

4.1.3.7. (*S*)-2-(4-Chlorobenzylideneamino)-3-hydroxy-*N*-tetradecylpropanamide (3g). Yield: 0.37 g (87%) as colorless powder. GC/MS (*m*/*e*): [422−H] M^+, ^{1}H NMR (DMSO-d_6, 300 MHz) δ/ppm = 8.264 (s, 1H), 7.870 (d, J = 7.8 Hz, 2H), 7.741 (t, J = 5.7 Hz, 1H), 7.506 (d, J = 7.8 Hz, 2H), 4.870 (t, J = 6 Hz, 1H), 3.809 (m, 2H), 3.463 (m, 1H), 3.065 (m, 2H), 1.382 (m, 2H), 1.188 (m, 22H), 0.829 (t, J = 6 Hz, 3H). ^{13}C NMR (DMSO-d_6, 75 MHz) δ/ppm = 170.360, 162.040, 136.198, 135.393, 130.747, 129.304, 76.193, 63.712, 39.054, 31.979, 29.732, 29.398, 26.983, 22.778, 14.609. Anal. Calcd for $C_{24}H_{39}ClN_2O_2$: C, 68.14; H, 9.29; N, 6.62; O, 7.56. Found: C 67.65; H, 9.76; N, 6.71; O, 7.93.

4.1.3.8. (*S*)-2-(3-Chlorobenzylideneamino)-3-hydroxy-*N*-tetradecylpropanamide (3h). Yield: 0.35 g (83%) as colorless powder. GC/MS (*m*/*e*): 423 M^+, 406 $[M-OH]^+$, ^{1}H NMR (DMSO-d_6, 300 MHz) δ/ppm = 8.257 (s, 1H), 7.979 (s, 1H), 7.767 (m, 2H), 7.502 (m, 2H), 4.851 (t, J = 6 Hz, 1H), 3.808 (m, 2H), 3.478 (m, 1H), 3.080 (m, 2H), 1.390 (m, 2H), 1.192 (m, 22H), 0.830 (t, J = 6 Hz, 3H). ^{13}C NMR (DMSO-d_6, 75 MHz) δ/ppm = 170.239, 161.888, 138.612, 134.254, 131.278, 131.126, 128.272, 128.014, 76.314, 63.742, 39.069, 31.979, 29.838, 29.717, 29.398, 27.014, 22.778, 14.609. Anal. Calcd for $C_{24}H_{39}ClN_2O_2$: C, 68.14; H, 9.29; N, 6.62; O, 7.56. Found: C 66.55; H, 9.20; N, 6.47; O, 8.81.

4.1.3.9. (*S*)-2-(2-Chlorobenzylideneamino)-3-hydroxy-*N*-tetradecylpropanamide (3i). Yield: 0.35 g (83%) as colorless powder. GC/MS (*m*/*e*): 423 M^+, ^{1}H NMR (DMSO-d_6, 300 MHz) δ/ppm = 8.603 (s, 1H), 8.185 (d, J = 7.5 Hz, 1H), 7.772 (t, J = 5.7 Hz, 1H), 7.465 (m, 3H), 4.868 (t, J = 6 Hz, 1H), 3.908 (dd, J = 3.9 Hz, J = 8.1 Hz, 1H), 3.802 (m, 1H), 3.478 (m, 1H), 3.083 (m, 2H), 1.390 (m, 2H), 1.194 (m, 22H), 0.834 (t, J = 6 Hz, 3H). ^{13}C NMR (DMSO-d_6, 75 MHz) δ/ppm = 170.117, 159.231, 137.260, 134.998, 133.131, 130.458, 129.487, 127.983, 76.421, 63.545, 39.069, 31.979, 29.717, 29.398, 26.999, 22.778, 14.624. Anal. Calcd for $C_{24}H_{39}ClN_2O_2$: C, 68.14; H, 9.29; N, 6.62; O, 7.56. Found: C, 67.80; H, 9.43; N, 6.69; O, 7.42.

4.1.3.10. (*S*)-2-(4-Methoxybenzylideneamino)-3-hydroxy-*N*-tetradecylpropanamide (3j). Yield: 0.36 g (86%) as colorless powder. GC/MS (*m*/*e*): 419 $[M+H]^+$, ^{1}H NMR (DMSO-d_6, 300 MHz) δ/ppm = 8.179 (s, 1H), 7.775 (d, J = 9.0 Hz, 2H), 7.680 (t, J = 5.7 Hz, 1H), 6.989 (d, J = 9.0 Hz, 2H), 4.814 (t, J = 6 Hz, 1H), 3.792 (s, 3H), 3.769 (m, 2H), 3.443 (m, 1H), 3.074 (m, 2H), 1.381 (m, 2H), 1.192 (m, 22H), 0.832 (t, J = 6 Hz, 3H). ^{13}C NMR (DMSO-d_6, 75 MHz) δ/ppm = 170.755, 162.465, 162.116, 130.732, 129.426, 114.576 76.178, 63.909, 55.984, 39.009, 31.979, 29.808, 29.717, 29.398, 26.983, 22.778, 14.624. Anal. Calcd for $C_{25}H_{42}N_2O_3$: C, 71.73; H, 10.11; N, 6.69; O, 11.47. Found: C 71.27; H, 10.10; N, 6.88; O, 11.80.

4.1.3.11. (*S*)-2-(3-Methoxybenzylideneamino)-3-hydroxy-*N*-tetradecylpropanamide (3k). Yield: 0.36 g (86%) as colorless powder. GC/MS (*m*/*e*): 419 $[M+H]^+$, ^{1}H NMR (DMSO-d_6, 300 MHz) δ/ppm = 8.234 (s, 1H), 7.719 (t, J = 5.7 Hz, 1H), 7.422 (s, 1H), 7.354 (m, 2H), 7.048 (m, 1H), 4.857 (t, J = 6 Hz, 1H), 3.790 (m, 5H), 3.480 (m, 1H), 3.081 (m, 2H), 1.364 (m, 2H), 1.192 (m, 22H), 0.833 (t, J = 6 Hz, 3H). ^{13}C NMR (DMSO-d_6, 75 MHz) δ/ppm = 170.482, 163.148, 160.142, 137.974, 130.306, 121.986, 117.659, 113.286, 76.284, 63.742, 55.893, 39.039, 31.979, 29.701, 29.398, 26.999, 22.778, 14.609. Anal. Calcd for $C_{25}H_{42}N_2O_3$: C, 71.73; H, 10.11; N, 6.69; O, 11.47. Found: C 71.21; H, 9.91; N, 6.95; O, 11.97.

4.1.3.12. (*S*)-2-(2-Methoxybenzylideneamino)-3-hydroxy-*N*-tetradecylpropanamide (3l). Yield: 0.30 g (72%) as colorless powder. GC/MS (*m*/*e*): 418 M^+, ^{1}H NMR (DMSO-d_6, 300 MHz) δ/ppm = 8.576 (s, 1H), 8.014 (d, J = 7.8 Hz, 1H), 7.698 (t, J = 5.7 Hz, 1H), 7.443 (t, J = 7.8 Hz, 1H), 7.089 (d, J = 7.8 Hz, 1H), 6.983 (t, J = 7.8 Hz, 1H), 4.796 (t, J = 6 Hz, 1H), 3.835 (s, 3H), 3.784 (m, 2H), 3.451 (m, 1H), 3.073 (m, 2H), 1.384 (m, 2H), 1.196 (m, 22H), 0.834 (t, J = 6 Hz, 3H). ^{13}C NMR (DMSO-d_6, 75 MHz) δ/ppm = 170.603, 159.291, 158.289, 133.161, 127.892, 124.355, 121.014, 112.375, 76.709, 63.818, 56.272, 39.009, 31.979, 29.808, 29.717, 29.398, 26.983, 22.778, 14.624. Anal. Calcd for $C_{25}H_{42}N_2O_3$: C, 71.73; H, 10.11; N, 6.69; O, 11.47. Found: C 71.33; H, 10.09; N, 6.68; O, 11.72.

4.1.4. General procedure for synthesis of hydroxy-substituted (*S*)-2-(benzylideneamino)-3-hydroxy-*N*-tetradecylpropanamide (3m–o)

A mixture of 0.40 g (1.00 mmol) of (*S*)-2-amino-3-hydroxy-*N*-tetradecylpropanamide hydrochloride, 0.04 g (1.00 mmol) of NaOH, 1.00 mmol of hydroxybenzaldehyde, and 40 mL of methanol was stirred at room temperature for eight hours. The solvent was then evaporated under reduced pressure, and the residue was washed with cold methanol to yield hydroxy-substituted (*S*)-2-(benzylideneamino)-3-hydroxy-*N*-tetradecylpropanamide as powder. Recrystallization was performed using petroleum ether/methanol.

4.1.4.1. (*S*)-2-(4-Hydroxybenzylideneamino)-3-hydroxy-*N*-tetradecylpropanamide (3m). Yield: 0.20 g (50%) as colorless powder. GC/MS (*m*/*e*): 404 M^+, 387 $[M-OH]^+$, ^1H NMR (DMSO-d_6, 300 MHz) δ/ppm = 8.114 (s, 1H), 7.639 (m, 3H), 6.806 (d, J = 8.1 Hz, 2H), 4.768 (t, J = 6 Hz, 1H), 3.739 (m, 2H), 3.429 (m, 1H), 3.070 (m, 2H), 1.381 (m, 2H), 1.201 (m, 22H), 0.834 (t, J = 6 Hz, 3H). ^{13}C NMR (DMSO-d_6, 75 MHz) δ/ppm = 170.846, 162.617, 160.734, 130.868, 127.953, 115.958, 76.132, 63.955, 39.994, 31.979, 29.797, 29.717, 29.382, 26.983, 22.778, 14.624. Anal. Calcd for $C_{24}H_{40}N_2O_3$: C, 71.25; H, 9.97; N, 6.92; O, 11.86. Found: C 71.22; H, 10.24; N, 6.86; O, 11.66.

4.1.4.2. (*S*)-2-(3-Hydroxybenzylideneamino)-3-hydroxy-*N*-tetradecylpropanamide (3n). Yield: 0.21 g (52%) as colorless powder. GC/MS (*m*/*e*): 387 $[M-OH]^+$, ^1H NMR (DMSO-d_6, 300 MHz) δ/ppm = 8.166 (s, 1H), 7.635 (t, J = 5.7 Hz, 1H), 7.235 (m, 3H), 6.860 (m, 1H), 3.783 (m, 2H), 3.464 (m, 1H), 3.075 (m, 2H), 1.385 (m, 2H), 1.202 (m, 22H), 0.834 (t, J = 6 Hz, 3H). ^{13}C NMR (DMSO-d_6, 75 MHz) δ/ppm = 170.497, 163.406, 158.365, 137.883, 130.170, 120.255, 118.782, 115.123, 76.223, 63.773, 39.039, 31.994, 29.853, 29.732, 29.413, 27.014, 22.793, 14.624. Anal. Calcd for $C_{24}H_{40}N_2O_3$: C, 71.25; H, 9.97; N, 6.92; O, 11.86. Found: C 71.20; H, 10.21; N, 6.83; O, 11.70.

4.1.4.3. (*S*)-2-(2-Hydroxybenzylideneamino)-3-hydroxy-*N*-tetradecylpropanamide (3o). Yield: 0.15 g (37%) as yellow powder. GC/MS (*m*/*e*): 403 $[M-H]^+$, 387 $[M-OH]^+$, ^1H NMR (DMSO-d_6, 300 MHz) δ/ppm = 8.468 (s, 1H), 7.924 (t, J = 5.7 Hz, 1H), 7.473 (d, J = 7.5 Hz, 1H), 7.322 (t, J = 7.5 Hz, 1H), 6.882 (m, 2H), 4.926 (br, 1H), 3.918 (dd, J = 4.5 Hz, J = 7.8 Hz, 1H), 3.777 (dd, J = 4.5 Hz, J = 10.8 Hz, 1H), 3.569 (m, 1H), 3.050 (m, 2H), 1.373 (m, 2H), 1.195 (m, 22H), 0.835 (t, J = 6 Hz, 3H). ^{13}C NMR (DMSO-d_6, 75 MHz) δ/ppm = 169.571, 167.278, 161.022, 133.115, 132.478, 119.587, 119.238, 117.127, 75.115, 63.408, 39.176, 31.979, 29.717, 29.656, 29.398, 26.983, 22.778, 14.624. Anal. Calcd for $C_{24}H_{40}N_2O_3$: C, 71.25; H, 9.97; N, 6.92; O, 11.86. Found: C 71.12; H, 10.06; N, 6.78; O, 12.00.

4.1.5. General procedure for synthesis substituted (*S*)-2-(benzylamino)-3-hydroxy-*N*-tetradecylpropanamide (4c, 4l, 4i, and 4o)

To the solution of 0.20 mmol substituted (*S*)-2-(benzylideneamino)-3-hydroxy-*N*-tetradecylpropanamides **3c**, **3l**, **3i**, and **3o** in 10 mL of methanol, 20 mg (0.54 mmol) of $NaBH_4$ was added. The reaction mixture was stirred at room temperature for 10 h, and evaporated under vacuum. The residue was purified by thin layer chromatography to give substituted (*S*)-2-(benzylamino)-3-hydroxy-*N*-tetradecylpropanamides **4c**, **4l**, **4i**, and **4o** as colorless powder in 73–78% yields.

4.1.5.1. (*S*)-2-(2-Nitrobenzylamino)-3-hydroxy-*N*-tetradecylpropanamide (4c). Yield: 75%, colorless powder. GC/MS (*m*/*e*): 435 M^+, 418 $[M-OH]^+$, ^1H NMR (DMSO-d_6, 300 MHz) δ/ppm = 7.926 (d, J = 3.6 Hz, 1H), 7.720 (m, 3H), 7.500 (t, J = 8.4 Hz, 1H), 4.720 (t, J = 5.4 Hz, 1H), 3.977 (d, J = 15.3 Hz, 1H), 3.847 (d, J = 15.3 Hz, 1H), 3.462 (m, 2H), 3.021 (m, 3H), 1.359 (m, 2H), 1.209 (m, 24H), 0.833 (t, J = 6.6 Hz, 3H). ^{13}C NMR (DMSO-d_6, 75 MHz) δ/ppm = 172.243, 137.245, 135.803, 133.844, 131.415, 128.834, 124.947, 64.608, 63.120, 48.741, 38.963, 31.979, 29.732, 29.671, 29.382, 27.014, 22.778, 14.609. Anal. Calcd for $C_{24}H_{41}N_3O_4$: C, 66.17; H, 9.49; N, 9.65; O, 14.69. Found: C, 66.60; H, 9.69; N, 9.54; O, 14.33.

4.1.5.2. (*S*)-2-(2-Chlorobenzylamino)-3-hydroxy-*N*-tetradecylpropanamide (4i). Yield: 73%, colorless powder. GC/MS (*m*/*e*): 424 M^+, ^1H NMR ($CDCl_3$, 300 MHz) δ/ppm = 7.404–7.233 (m, 5H), 3.899 (s, 2H), 3.794 (t, J = 5.1 Hz, 2H), 3.237 (t, J = 5.7 Hz, 3H), 1.633 (m, 2H), 1.492 (t, J = 6.9 Hz, 2H), 1.257 (m, 24H), 0.882 (t, J = 6.9 Hz, 3H). ^{13}C NMR ($CDCl_3$, 75 MHz) δ/ppm = 136.319, 130.641, 130.048, 129.168, 127.270, 114.971, 63.180, 62.922, 50.639, 39.312, 32.145, 29.868, 29.762, 29.579, 29.504, 27.150, 22.899, 14.335. Anal. Calcd for $C_{24}H_{41}ClN_2O_2$: C, 67.82; H, 9.72; N, 6.59; O, 7.53. Found: C, 67.58; H, 9.93; N, 6.69; O, 9.72.

4.1.5.3. (*S*)-2-(2-Methyoxybenzylamino)-3-hydroxy-*N*-tetradecylpropanamide (4l). Yield: 78%, colorless powder. GC/MS (*m*/*e*): 319 $[M-H]^+$, ^1H NMR ($CDCl_3$, 300 MHz) δ/ppm = 7.359–6.906 (m, 5H), 4.076 (dd, J = 3.0 Hz, J = 11.1 Hz, 1H), 3.855 (s, 3H), 3.758 (m, 2H), 3.590 (m, 1H), 3.250 (m, 2H), 2.247 (m, 1H), 1.501 (m, 2H), 1.254 (m, 24H), 0.880 (t, J = 6.9 Hz, 3H). ^{13}C NMR ($CDCl_3$, 75 MHz) δ/ppm = 136.319, 130.641, 130.048, 129.168, 127.270, 114.971, 63.180, 62.922, 52.203, 50.639, 39.312, 32.145, 29.868, 29.762, 29.579, 29.504, 27.150, 22.899, 14.335. Anal. Calcd for $C_{25}H_{44}N_2O_3$: C, 71.39; H, 10.54; N, 6.66; O, 11.41. Found: C, 71.30; H, 9.82; N, 6.90; O, 11.81.

4.1.5.4. (*S*)-2-(2-Hydroxybenzylamino)-3-hydroxy-*N*-tetradecylpropanamide (4o). Yield: 75%, colorless powder. GC/MS (*m*/*e*): 405 $[M-H]^+$, 389 $[M-OH]^+$,^1H NMR ($CDCl_3$, 300 MHz) δ/ppm = 7.188 (t, J = 7.5 Hz, 1H), 6.985 (d, J = 7.5 Hz, 1H), 6.846 (d, J = 7.5 Hz, 1H), 6.799 (t, J = 7.5 Hz, 1H), 6.196 (br, 1H), 4.090 (d, J = 14.1 Hz, 1H), 3.839 (m, 2H), 3.757 (dd, J = 5.4 Hz, J = 11.1 Hz, 1H), 3.281 (m, 2H), 3.142 (t, J = 5.4 Hz, 1H), 1.513 (t, J = 6.6 Hz, 2H), 1.262 (m, 24H), 0.882 (t, J = 6.6 Hz, 3H). ^{13}C NMR ($CDCl_3$, 75 MHz) δ/ppm = 159.003, 129.396, 129.198, 122.335, 119.815, 116.702, 62.953, 61.283, 50.578, 39.859, 32.145, 29.868, 29.807, 29.716, 29.579, 29.473, 27.089, 22.899, 14.335. Anal. Calcd for $C_{24}H_{42}N_2O_3$: C, 70.89; H, 10.41; N, 6.89; O, 11.80. Found: C, 70.29; H, 10.99; N, 6.86; O, 11.92.

4.2. Bioassays

4.2.1. Cell culture

Human cancer cell lines derived from breast, MCF-7TN-R were cultured in 75 cm^2 culture flasks in DMEM (Invitrogen, Co., Carlsbad, CA) supplemented with 10% FBS (Life Technologies, Inc., Gaithersburg, MD), basic minimum MEM essential (50×, Invitrogen Co.) and MEM non-essential (100×, Invitrogen, Co.) amino acids, sodium pyruvate (100× Invitrogen Co.), antimycotic–antibiotic (10,000 U/mL penicillin G sodium; 10,000 μg/mL streptomycin sulfate; 25 μg/mL amphotericin B as Fungizone®), and human recombinant insulin (4 mg/mL. Invitrogen Co). Culture flasks were maintained in a tissue culture incubator in a humidified atmosphere of 5% CO_2 and 95% air at 37 °C.

4.2.2. MTT viability assay

MCF-7TN-R cells were plated at 7.5×10^5 cells per well in a 96-well plate in phenol-free DMEM supplemented with 5% FBS and allowed to adhere overnight. Cells were then treated with

analogs **3a–o** (ranging from 0.1 to 100 μM) for 24 h. Following treatment, 20 mL of MTT (5 mg/mL) reagent was incubated in each well for 4 h. Cells were then lysed with 20% SDS in 50% dimethylformamide. The pH and absorbances are read on an ELx808 Microtek plate reader (Winooski, VT) at 550 nm, with a reference wavelength of 630 nm. The values are the mean of ±SE of four independent experiments. The same protocol was used for the MTT assays on HEK294 non-tumorigenic human kidney cell line.

4.2.3. Statistical analysis

Statistical analysis of IC_{50} values were calculated from concentration-response curves using GraphPad Prism 5.0 (Graphpad Software, San Diego, CA), using with the equation:

$$Y = \text{Bottom} + (\text{Top} - \text{Bottom})/1 + 10\,\text{Log}\,\text{EC50} - X.$$

Assuming a standard slope, where the response goes from 10% to 90% of maximal as X increases over two log units. Differences in IC_{50} were compared using Student's unpaired t-test with $p<0.05$ as the limit of statistical significance. Experiments comparing multiple concentrations to the control will be tested with one-way ANOVA with Bonferroni post-test to compare individual concentrations. All statistical analysis will be done using GraphPad Prism 5.0.

4.3. Determination of Log *K* of 3a–o

Substituted (S)-2-(benzylideneamino)-3-hydroxy-N-tetradecylpropanamides **3a-o** were dissolved in aqueous to prepare sample solutions of 15 μM. The RP-HPLC analysis was carried out on *hp* Hewlett Packard Series 1050 (phenomenex Gemini-NX 5u C18 110A). After 5 μL of the sample was loaded, the column was eluted with a solution consisting of CH_3OH/H_2O 85:15 (v/v) as the mobile phase for 30 min. The flow rate was 1 mL/min. The peak of **3a–o** in the sample was monitored with UV detector at 254.40 nm (550.10 nm for reference) and the retention time (t_R) corresponding to its peak was recorded. With the same HPLC conditions, the retention time of acetone peak was recorded as dead time t_0. In order to offset the influence of the solvent on the appearance time of the peak of **3a–o**, the appearance time of acetone peak (t_0, 1.556 min) was used as a control. As an alternative representation of t_R, Log K was defined based on the equation $\text{Log}\,K = \text{Log}\,[(t_R - t_0)/t_0]$.

Acknowledgements

This research was supported by a grant from the Louisiana Cancer Research Consortium (#631324). We thank Ms. Xiaoyi Zhang and Beijing Area Major Laboratory of Peptide and Small Molecular Drugs (IHLB, KZ200810025010) for their assistance in computational chemistry.

References and notes

1. Hannun, Y. A.; Obeid, L. M. *Nat. Rev. Mol. Cell Biol.* **2008**, *9*, 139.
2. Saddoughi, S. A.; Song, P.; Ogretmen, B. *Subcell Biochem.* **2008**, *49*, 413.
3. Schiffmann, S.; Sandner, J.; Birod, K.; Wobst, I.; Angioni, C.; Ruckhaberle, E.; Kaufmann, M.; Ackermann, H.; Lotsch, J.; Schmidt, H.; Geisslinger, G.; Grosch, S. *Carcinogenesis* **2009**, *30*, 745.
4. Pettus, B. J.; Chalfant, C. E.; Hannun, Y. A. *Biochim. Biophys. Acta* **2002**, *1585*, 114.
5. Webb, L. M.; Arnholt, A. T.; Venable, M. E. *Mol. Cell Biochem.* **2010**, *337*, 153.
6. Modrak, D. E.; Leon, E.; Goldenberg, D. M.; Gold, D. V. *Mol. Cancer Res.* **2009**, *7*, 890.
7. Bourbon, N. A.; Sandirasegarane, L.; Kester, M. *J. Biol. Chem.* **2002**, *277*, 3286.
8. Mathew, T.; Cavallari, M.; Billich, A.; Bornancin, F.; Nussbaumer, P.; De Libero, G.; Vasella, A. *Chem. Biodivers.* **2009**, *6*, 1688.
9. Antoon, J. W.; Liu, J.; Gestaut, M. M.; Burow, M. E.; Beckman, B. S.; Foroozesh, M. *J. Med. Chem.* **2009**, *52*, 5748.
10. Bai, A.; Szulc, Z. M.; Bielawski, J.; Mayroo, N.; Liu, X.; Norris, J.; Hannun, Y. A.; Bielawska, A. *Bioorg. Med. Chem.* **2009**, *17*, 1840.
11. Macchia, M.; Barontini, S.; Bertini, S.; Di Bussolo, V.; Fogli, S.; Giovannetti, E.; Grossi, E.; Minutolo, F.; Danesi, R. *J. Med. Chem.* **2001**, *44*, 3994.
12. Struckhoff, A. P.; Bittman, R.; Burow, M. E.; Clejan, S.; Elliott, S.; Hammond, T.; Tang, Y.; Beckman, B. S. *J. Pharmacol. Exp. Ther.* **2004**, *309*, 523.
13. Antoon, J. W.; Liu, J.; Ponnapakkam, A. P.; Gestaut, M. M.; Foroozesh, M.; Beckman, B. S. *Cancer Chemother. Pharmacol.* **2010**, *65*, 1191.
14. Lim, H. S.; Oh, Y. S.; Suh, P. G.; Chung, S. K. *Bioorg. Med. Chem. Lett.* **2003**, *13*, 237.
15. Gududurru, V.; Hurh, E.; Durgam, G. G.; Hong, S. S.; Sardar, V. M.; Xu, H.; Dalton, J. T.; Miller, D. D. *Bioorg. Med. Chem. Lett.* **2004**, *14*, 4919.
16. Bieberich, E.; Kawaguchi, T.; Yu, R. K. *J. Biol. Chem.* **2000**, *275*, 177.
17. Bedia, C.; Canals, D.; Matabosch, X.; Harrak, Y.; Casas, J.; Llebaria, A.; Delgado, A.; Fabrias, G. *Chem. Phys. Lipids* **2008**, *156*, 33.
18. Grijalvo, S.; Bedia, C.; Triola, G.; Casas, J.; Llebaria, A.; Teixido, J.; Rabal, O.; Levade, T.; Delgado, A.; Fabrias, G. *Chem. Phys. Lipids* **2006**, *144*, 69.
19. Weldon, C. B.; Parker, A. P.; Patten, D.; Elliott, S.; Tang, Y.; Frigo, D. E.; Dugan, C. M.; Coakley, E. L.; Butler, N. N.; Clayton, J. L.; Alam, J.; Curiel, T. J.; Beckman, B. S.; Jaffe, B. M.; Burow, M. E. *Int. J. Oncol.* **2004**, *24*, 1473.
20. Abraham, R. J.; Grant, G. H.; Haworth, I. S.; Smith, P. E. *J. Comput. Aided Mol. Des.* **1991**, *5*, 21.
21. Baba, A.; Yoshioka, T. *Chem. Res. Toxicol.* **2009**, *22*, 1998.
22. Mittal, R. R.; Harris, L.; McKinnon, R. A.; Sorich, M. J. *J. Chem. Inf. Model.* **2009**, *49*, 704.
23. Gieleciak, R.; Polanski, J. *J. Chem. Inf. Model.* **2007**, *47*, 547.